Materials Science-Poland, 41(3), 2023, pp. 62-73
http://www.materialsscience.pwr.wroc.pl/
DOI: 10.2478/msp-2023-0034

Eco-friendly high-rate formation of silver nanoparticles in agave inulin and its bactericidal effect against *Escherichia coli*

María Teresa Sánchez-Vieyra[1], Miguel Ojeda-Martínez[1], Eden Oceguera-Contreras[2], Sergio Yair Rodríguez-Preciado[2], Mariana Díaz-Zaragoza[2], Brenda Esmeralda Martínez-Zérega[3], José Luis González-Solís[3], David Omar Oseguera-Galindo[1,*]

[1]Universidad de Guadalajara, Centro Universitario de los Valles, Dpto. Cs. Naturales y Exactas, Carretera Guadalajara-Ameca Km 45.5, Ameca, Jalisco, México, 46600

[2]Universidad de Guadalajara, Centro Universitario de los Valles, Dpto. Cs. Salud, Carretera Guadalajara-Ameca Km 45.5, Ameca, Jalisco, México, 46600

[3]Universidad de Guadalajara, Centro Universitario de los Lagos, Laboratorio de Biofísica y Ciencias Biomédicas, Enrique Díaz de León, Paseo de la Montaña, Lagos de Moreno, Jalisco, México, 47460

A high rate of silver nanoparticle formation, effective against the *Escherichia coli* (*E. coli*) bacterium, was obtained for the first time by means of a simple, eco-friendly, and low-cost green method in a solution of agave inulin. The study was carried out using the traditional method, in which the effects of the concentration of agave inulin, $AgNO_3$, temperature, and pH on the synthesis were analyzed by UV-Vis spectroscopy and transmission electron microscopy (TEM). Most of the nanoparticles produced were spherical with a size less than 10 nm. In a sample with 20 mg/mL of agave inulin, 1 mM of $AgNO_3$, T = 23°C, and pH = 12, the highest percentage of Ag^+ ions available in the solution were reduced for the formation of nanoparticles in less than 40 min, whereas a sample prepared with 60 mg/mL of agave inulin, 10 mM of $AgNO_3$, T = 23°C, pH = 12, and a storage time of 40 min showed a significant bactericidal effect on the *E. coli* strain. Agave inulin is a good biological compound for the formation of small, spherical silver nanoparticles. A pH of 12 favors a higher production speed of the silver nanoparticles and better use of the available Ag^+ ions. In addition to this, the concentration of $AgNO_3$ is a determining factor for increased formation of the nanoparticles necessary to bactericidal effect.

Keywords: *silver nanoparticles, green synthesis, agave inulin, absorbance, bactericidal effect*

1. Introduction

The bactericidal effect of silver nanoparticles (AgNPs), presented in the nanoscale range, has potential applications in areas such as health, medicine, and agriculture [1, 2]; and many studies have been performed based on chemical, physical, and green synthesis methods [3]. However, green synthesis is getting special attention for being a simple, eco-friendly, and low-cost method of synthesizing silver nanoparticles [4, 5].

In 2003, the preparation of silver nanoparticles using a type of plant, particularly an alfalfa plant, was reported for the first time in 2003 by Gardea et al. [6]. Since then, many articles have reported different plants, leaves, and seeds as synthesis medium [7, 8]. Green methods of silver nanoparticle synthesis consist of dilute silver nitrate ($AgNO_3$) as a precursor of silver ions (Ag^+) in a natural extract, where the biological molecules play an important role as a reducing and stabilizing agent, favoring nanoparticle formation [9].

Agave inulin is a reducing sugar, obtained from agave pineapples, which are widely cultivated in Jalisco, México [10]. It consists of a chain of 2 to 60 fructose molecules terminated at the reducing end with glucose. Its monosaccharides are linked by β(2-1) glycosidic bonds terminated at the reducing end by an α-D-(1-2)-glucopyranoside [11]. Agave inulin was recently shown to successfully

* E-mail: david.oseguera@academicos.udg.mx

contribute to reducing and stabilizing the formation of silver nanoparticles [12]. In addition, because of its physicochemical properties, it has a wide number of applications in the food, pharmaceutical, and chemical industries [13–16].

Among the desirable characteristics for the synthesis of silver nanoparticles is the rate formation, which is associated with the nanoparticle concentration and is a value that has an effect on a specific application. For instance, in order to study antibacterial activity, in addition to the size and the shape of the nanoparticles, it is important to use an adequate concentration of AgNPs [17, 18].

Usually, to study the rate formation of AgNPs, UV-Vis spectrophotometry is used to measure the maximum absorbance around 400 nm. Furthermore, the linear relation from Lambert-Beer (Eq. 1):

$$A = \alpha l C \tag{1}$$

where A is the absorbance, α is the absorption coefficient, l is the path radiation length through the sample, and C is the concentration of suspended nanoparticles in the absorbent, indicate that a higher concentration of nanoparticles in suspension corresponds to a larger absorbance peak, and an increase in the absorbance peak means that the nanoparticle formation also increased [19].

Nevertheless, in agreement with the Mie theory, if the absorption peak is shifted toward a larger wavelength, this suggests changes in the size of the nanoparticles [20].

Either the formation rate or the nanoparticle concentration could be affected by some experimental factors including salt concentration, natural extract concentration, reaction temperature, and pH of the solution. For instance, after measuring the absorbance of silver AgNPs in *Alcalypha indica* leaf extract, the authors concluded that with an alkaline pH (9 and 11) rapid nanoparticle formation occurs [21]. Moreover, similar results were reported for using *Calendula Officinalis* seed extract, the sample prepared with a pH of 9 and the sample with a temperature of 60°C registered a maximum absorption [22].

In addition, when AgNPs were synthesized in a neem leaf extract with a different pH (9–13), rapid formation of nanoparticles was evident in a few minutes. As the pH increased, the absorption peak increased too, and it shifted towards a longer wavelength, indicating an increase in the size of synthesized AgNPs [23]. Similar results were reported in nanoparticles using leaf extracts of *Ocimum sanctum* (Tulsi) and its derivative quercetin to different pH levels (pH 7, 8, 9, 10, and 11) [24].

In this work, we present results of the formation of silver nanoparticles by means of a green method using agave inulin as a reducing and stabilizing agent. The effect of agave inulin concentration, $AgNO_3$ concentration, temperature, and pH on the production of silver nanoparticles is studied. Furthermore, a theoretical estimate of the highest concentration of AgNPs produced is made and its bactericidal effect on the *E. coli* bacterium is analyzed.

2. Experimental methods

The optimization of nanoparticle synthesis was carried out using the traditional method, which consists of monitoring the influence of one variable at a time in an experimental response, that is, when only one parameter is changed, and the others remain constant [25]. In this study, agave inulin concentration, $AgNO_3$ concentration, temperature, and pH are the variables used in the synthesis of AgNPs.

The agave inulin was acquired from the EDULAG company (Jalisco, México) in powder form, and silver nitrate salt ($AgNO_3$) and sodium hydroxide (NaOH) were acquired from the Sigma Aldrich company.

Prepared samples were kept at room temperature (23°C), except when the effect of temperature was explored, and the samples were duplicated to ensure reproducibility. All samples were covered with aluminum foil and kept in complete rest in the dark. Distilled water was used in all samples, reaching a total volume of 50 mL in each solution.

The monitoring of the absorption spectra of the samples was done with a Genesys 150 UV-Vis spectrophotometer. Nanoparticles were observed with a transmission electron microscope (TEM), JeolJem-2010.

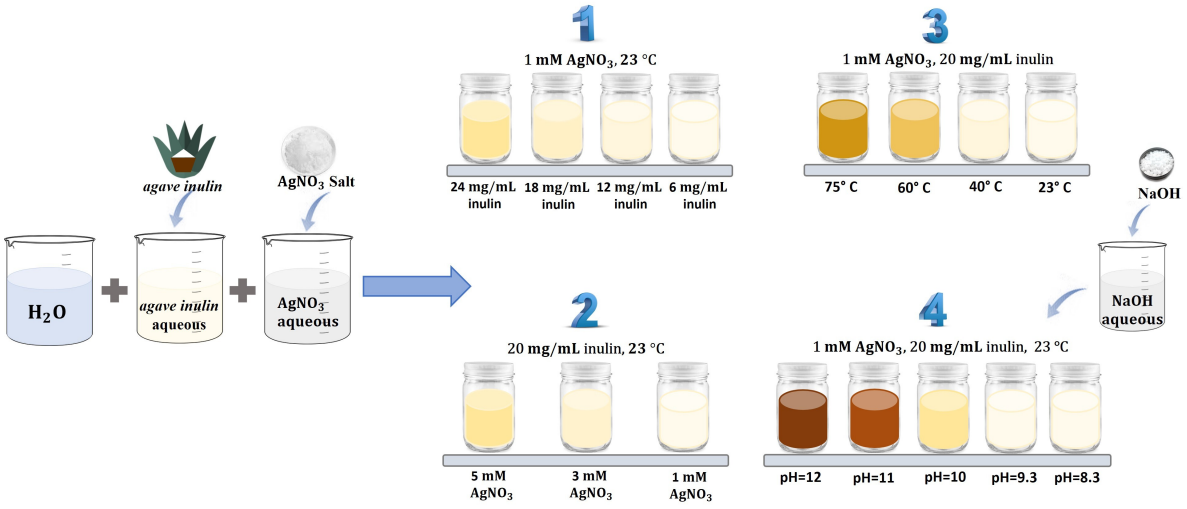

Fig. 1. Experimental setup for the synthesis of AgNPs. Variables were (1) agave inulin; (2) $AgNO_3$; (3) temperature; (4) pH

The micrographs were prepared using Adobe Photoshop software, then, with ImageJ software, the areas of nanoparticles within pixels were measured and their diameters in nanometers were determined considering the area measured as a circle. Finally, with the Origin program, size distributions were prepared. The distributions were fitted with a log-normal distribution function as defined in Equation (2) with mean $\bar{x}$ and multiplicative standard deviation σ.

$$f(x) = \frac{A}{\sigma x\sqrt{2\pi}} e^{-\frac{\left(\ln\left(\frac{x}{\bar{x}}\right)\right)^2}{2\sigma^2}} \qquad (2)$$

Figure 1 shows a scheme of four experiments with different variables (1) inulin concentration (24, 18, 12, 6 mg/mL); (2) $AgNO_3$ concentration (5, 3, 1 mM); (3) temperature ((75°C, 60°C, 40°C, 23°C); (4) and pH (12, 11, 10, 9.3, 8.3). In the fourth experiment, in order to adjust the pH in each sample, a molar concentration of 0.1 M sodium hydroxide (NaOH) was prepared and meticulously added in drops to the solution of *agave inulin* until it reached the desired pH value, then the $AgNO_3$ solution was added. In the third experiment, the temperature of the agave inulin was adjusted by placing the solution on a hot plate with magnetic stirring, and when the solution reached the desired temperature, the $AgNO_3$ solution was added. The sample was kept at the desired temperature for 1 hour, and then it was removed from the magnetic stirring plate and allowed to cool to room temperature.

2.1. Effect of agave inulin on the synthesis

Four samples (S1A, S2A, S3A, S4A) with different agave inulin concentrations and the same $AgNO_3$ concentration, the same temperature, and the same pH were prepared. Table 1 shows the synthesis parameters and the corresponding values used. These samples were analyzed by UV-Vis spectroscopy 23 days after the preparation.

2.2. Effect of $AgNO_3$ on the synthesis

Three samples (S1B, S2B, S3B) with different $AgNO_3$ concentrations and the same *agave inulin* concentration, value of temperature, and pH were

Table 1. Parameters and values used in the preparation of samples to study agave inulin's effect on the synthesis of AgNPs

Sample	A	B	C	D
S1A	6	1	23	6.5
S2A	12	1	23	6.5
S3A	18	1	23	6.5
S4A	24	1	23	6.5

A: *agave inulin* (mg/mL); B: $AgNO_3$ (mM); C: temperature (°C); D: pH.

Table 2. Parameters and values used in the preparation of samples to study the $AgNO_3$ effect on the synthesis of AgNPs

Sample	A	B	C	D
S1B	20	1	23	6.5
S2B	20	3	23	6.5
S3B	20	5	23	6.5

A: *agave inulin* (mg/mL); B: $AgNO_3$ (mM); C: temperature (°C); D: pH.

prepared. Table 2 shows the parameters and their corresponding values used in the synthesis. The samples were analyzed by UV-Vis spectroscopy 22 days after the preparation.

2.3. Effect of temperature on the synthesis

Four samples (S1C, S2C, S3C, S4C) with different temperature values and the same *agave inulin* concentration, $AgNO_3$ concentration, and pH were synthesized. Table 3 shows the parameters and their corresponding values used for the synthesis. The samples were analyzed by UV-Vis spectroscopy 11 days after the preparation. The sample obtained with a temperature of 75°C was analyzed by TEM.

2.4. Effect of pH on the synthesis

Five samples (S1D, S2D, S3D, S4D, S5D) with different pH values and the same agave inulin concentration, $AgNO_3$ concentration, and temperature were prepared. Table 4 shows the parameters and the corresponding values used in the synthesis. The samples were analyzed by UV-Vis spectroscopy 40 min after the preparation. The samples S3D (pH = 10) and S2D (pH = 11) were characterized by TEM.

Table 3. Parameters and values used in the preparation of samples to study temperature effect on the synthesis of AgNPs

Sample	A	B	C	D
S1C	20	1	23	6.5
S2C	20	1	40	6.5
S3C	20	1	60	6.5
S4C	20	1	75	6.5

A: *agave inulin* (mg/mL); B: $AgNO_3$ (mM); C: temperature (°C); D: pH.

Table 4. Parameters and values used in the preparation of samples to study pH effect on the synthesis of AgNPs

Sample	A	B	C	D
S1D	20	1	23	12
S2D	20	1	23	11
S3D	20	1	23	10
S4D	20	1	23	9.3
S5D	20	1	23	8.3

A: *agave inulin* (mg/mL); B: $AgNO_3$ (mM); C: temperature (°C); D: pH.

2.5. Antibacterial activity of silver nanoparticles

The bactericidal effect of silver nanoparticles was determined using a strain of *E. coli*. This bacterium was extracted from Ameca's river (located in Jalisco, Mexico), and a bacterial culture was characterized in a chromogenic agar (CHROMOgar) and by PCR to confirm its presence by malB gene amplification. Subsequently, the bacterium was exposed to two different nanoparticle concentrations labeled $S1_{bac}$ and $S2_{bac}$. The first sample of nanoparticles ($S1_{bac}$) was synthesized using a 10 mM of $AgNO_3$ in solution with agave inulin at a concentration of 60 mg/mL. The second sample ($S2_{bac}$) was synthesized using 1 mM of $AgNO_3$ in solution with agave inulin at a concentration of 20 g/mL. Both samples were prepared with a pH of 12.

To determine the antibacterial activity of the nanoparticles, the micro dilution method was employed [26]. Table 5 shows the content of each of the test tubes. The six tubes each contained 5 mL of Luria Bertani (LB) broth. Tubes 2–6 contained 100 μL of the bacterial culture at a concentration of 10^8 CFU/mL. In tube 3, 100 μL of agave inulin was added to reach a concentration of 60 mg/mL, and in tube 6 100 μL of agave inulin was added to the broth to reach a concentration of 20 mg/mL to verify the absence of an antibacterial effect by agave inulin. Finally, instead of agave inulin solution, tubes 4 and 5 received 100 μL of silver nanoparticles corresponding to the samples

Table 5. Contents of the test tubes to study antibacterial activity

Tube	LB (mL)	*E. coli* (μL)	Inulin (μL)	Sample (μL)
1	5	–	–	–
2	5	100	–	–
3	5	100	100	–
4	5	100	–	$S1_{bac}$ (100)
5	5	100	–	$S2_{bac}$ (100)
6	5	100	100	–

$S1_{bac}$ and $S2_{bac}$, respectively. The tubes were incubated at 37°C for 18–24 h, and the antibacterial effect was detected by the unaided eye.

3. Results and discussion

3.1. Effect of agave inulin on the synthesis

Figure 2 presents UV-Vis absorption spectra of the samples prepared with different agave inulin concentration. Details of the mixing proportions are shown in Table 1 (in the experimental section), 23 days after the preparation. The samples S2A, S3A, and S4A exhibited an absorption peak at 442, 440, and 439 nm, respectively, and this indicates that quasi-spherical AgNPs were formed [27]. Nevertheless, for the sample S1A, with less agave inulin, the absorption peak did not appear, suggesting insufficient or null nanoparticle formation. This occurred even though S1A had the same molar concentration of $AgNO_3$ as the rest of these samples; therefore, we can say that the concentration of agave inulin molecules plays a key role in nanoparticle formation.

The hydrolysis of agave inulin is relatively stable at room temperature and neutral pH, so upon the addition of water, the inulin chain undergoes cleavage of the glycosidic bonds and finally breaks down into its monosaccharides [14]. This leads to hydroxyl ion formation, favoring the reduction of Ag^+ ions [28]. The natural polysaccharide has been considered to contribute in the reduction and stabilization of AgNPs [29].

In addition, as can be seen in Figure 2, there are some differences in the spectra. The nanoparticles obtained using a higher concentration of agave inulin influenced the amplification of the absorption peak. In agreement with the Lambert-Beer relation, Equation (1), this can be associated with an increase in nanoparticle concentration. Furthermore, the absorption peak shifts slightly toward shorter wavelengths, suggesting a slight decrease in nanoparticle size.

3.2. Effect of $AgNO_3$ on the synthesis

Figure 3 shows the UV-Vis absorption spectra of the samples prepared with different $AgNO_3$ concentrations. Details of the mixing proportions are shown in Table 2 (in the experimental section), after measuring the absorbance 22 days after the preparation. Similarly, $AgNO_3$ concentrations had an effect on the intensification and in shifting the

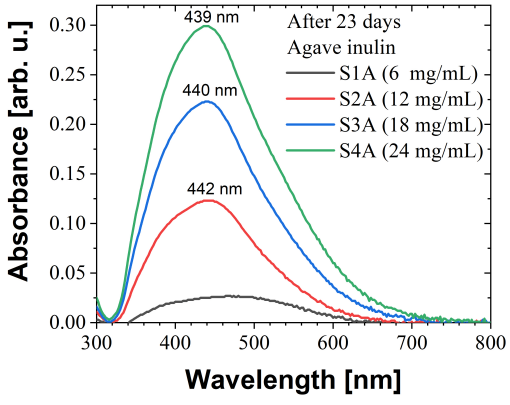

Fig. 2. UV-Vis absorbance of nanoparticles obtained using different agave inulin concentrations

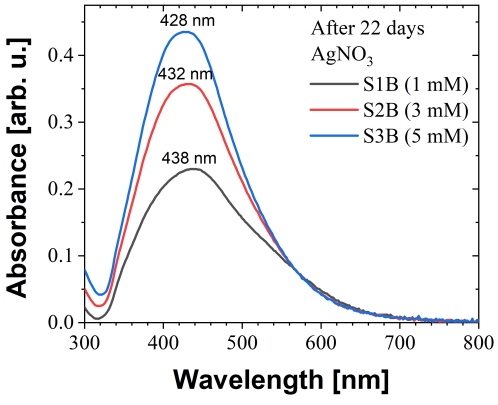

Fig. 3. UV-Vis absorbance of nanoparticles obtained using different $AgNO_3$ concentration

absorption peak to shorter wavelengths. This can be explained by the effect of the concentration and by a decrease in the nanoparticle size [9].

3.3. Effect of temperature on the synthesis

Figure 4 presents the UV-Vis absorption spectra corresponding to the samples obtained with different temperatures. Details of the mixing proportions are shown in Table 3 (in the experimental section) measuring the absorbance 11 days after the preparation. Samples S1C and S2C show less absorption around 400 nm; hence, there is little formation of AgNPs.

By contrast, sample S3C, obtained at 60°C, shows a more intense absorption peak. However, at 75°C, the sample S4C presents an absorption peak that is still more intense. Its absorbance value is the highest in comparison with the results presented in Figures 2 and 3. Hence, temperature influenced the acceleration of the nanoparticle formation.

In addition, Figure 5 presents the corresponding size distribution fitted with the log-normal model and micrographs of nanoparticles obtained with a temperature of 75°C (sample S4C). In this analysis, 354 particles were considered, where most of the nanoparticles exhibit a relatively small size of <10 nm with an average size of 7.99 nm. In agreement with the micrographs, the nanoparticles presented a quasi–spherical shape. This result reinforces the interpretation inferred from the profile of the absorption on the basis of the nanoparticle shape.

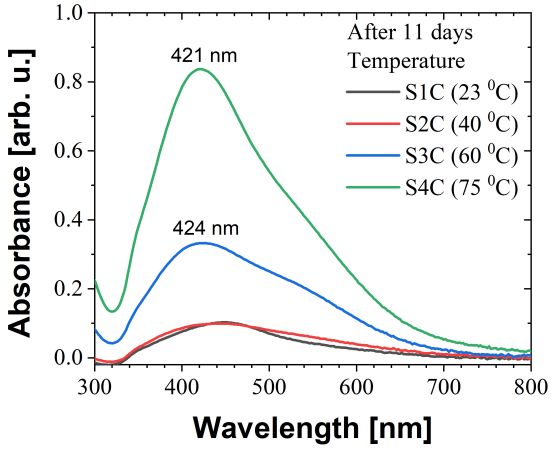

Fig. 4. UV-Vis absorbance of nanoparticles obtained using different temperatures

3.4. Effect of pH on the synthesis

Figure 6 presents UV-Vis absorption spectra of the samples obtained with different pHs; details of the mixing proportions are shown in Table 4 (in the experimental section). The absorption peak became more intense as pH increased. In fact, within the first forty minutes, the sample with a pH of 11 showed an absorbance of 1.7, whereas the sample with the highest pH had an absorption peak so intense that it exceeded the measurable range and its center could not be observed. In comparation with the other parameters used here, this indicates that a pH of 12 has more of an effect on the acceleration of nanoparticle formation. This result also correlates with the sample's dark color and the resulting difficulty in measuring light transmission.

Regarding the non-definition of this absorption peak, it was monitored while diluting the sample with distilled water with the following dilutions of distilled water to silver nanoparticles: 1:1, 2:1, 3:1, 4:1 and 5:1, where the first number is milliliters of distilled water diluting 1 milliliter of silver nanoparticles solution (the second number) in every case. Figure 7(a) shows the UV-Vis spectra of this monitoring. The absorbance decreases with the dilution with distilled water, showing that, despite the impossibility of observing its absorption peak, it is possible to recover the profile of the absorption peak generated by the diluted silver nanoparticles and thus identifying the center of its absorbance maximum, which is 402 nm. In this way, it can be observed that the absorption peak shifted towards a shorter wavelength (from 432 to 402) by means of increasing the pH (see Figures 6 and 7a), suggesting that the nanoparticle size decreases with the pH.

To understand the scope of the maximum absorbance of the original sample, absorbance monitoring allowed us to generate a calibration line, as seen in Figure 7(b). In this linear regression plot, an absorbance of 11.9 was calculated. Furthermore, since the sample was diluted into 3:1, 4:1, and 5:1, the profile of its absorption peak is similar. On the other hand, the linear regression predicts

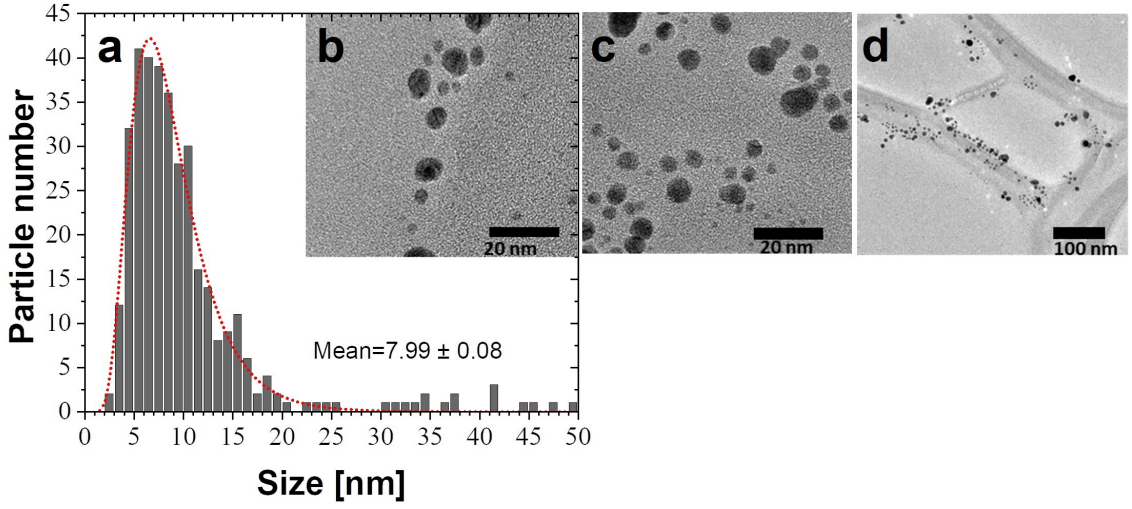

Fig. 5. (a) Size distribution, fitted with a Log-normal model (dotted line) from several micrographs (for instance b, c, and d) of AgNPs obtained using a temperature of 75°C

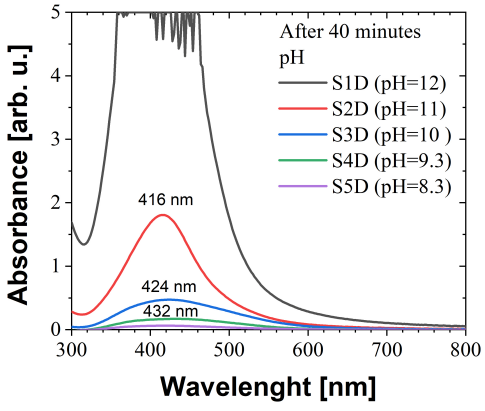

Fig. 6. UV-Vis absorbance of nanoparticles obtained using different pH values

with an acceptable precision the absorbance monitoring by UV-Vis spectroscopy.

In addition, Figure 8 presents a size distribution of the sample obtained using a pH of 11 (Sample S2D), there being 282 nanoparticles considered in the statistic, resulting in an average size of 6.04 nm. On the other hand, Figure 9 presents the size distribution of the sample obtained using a pH of 10 (Sample S3D), with 311 nanoparticles considered, resulting in an average size of 8.03 nm. The size distribution of nanoparticles obtained with a pH of 11 is narrower and presents the smallest nanoparticles. This result is similar to the work in which the authors published the effect of pH on the synthesis of AgNPs using citric and malic acids and reporting that the average size of the quasi-spherical nanoparticles decreases in a pH of 10 to 11 [30].

NaOH plays an important role in the intensification of the rate of nanoparticle formation. NaOH is a strong base that dissociates completely in solution to form hydroxyl ions [31]. Then, a large amount of these ions in an aqueous solution of inulin leads to an increment in its pH, which directly influences a notable increase in the speed of breaking the glycosidic bonds that join the fructose units that make up inulin [14]. Subsequently, as there is a greater number of fructose units, in consequence, there is a greater number of reducing molecules that immediately tend to give electrons to the Ag^{+} ions being reduced to Ag^{0} and consequently there is a rapid formation of silver nanoparticles.

A second important factor is the temperature. Nanoparticle preparation can be simpler without adjusting the pH and its temperature, and only using ingredients such as agave inulin, $AgNO_3$, and distilled water. Although it is very important

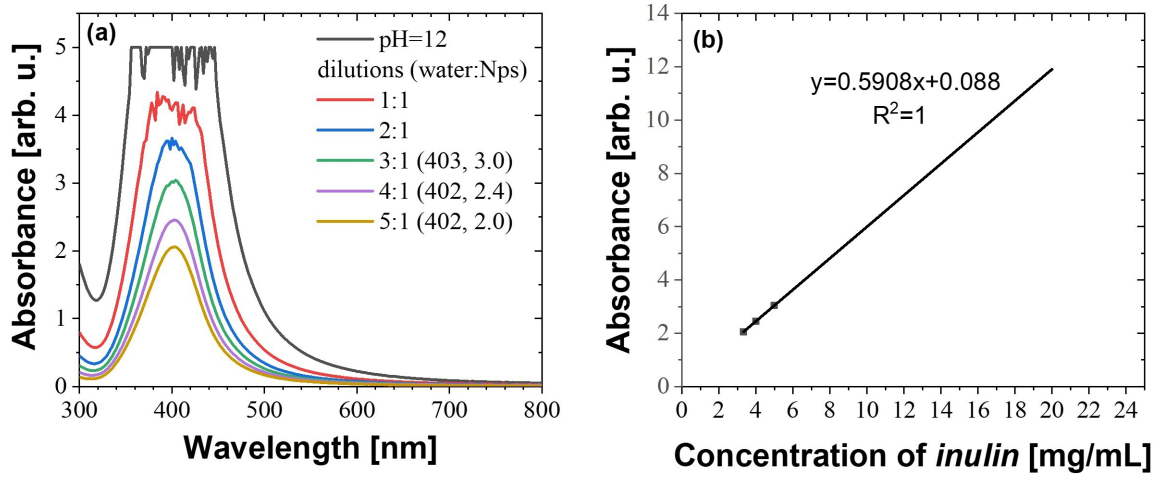

Fig. 7. (a) UV-Vis spectra of nanoparticles obtained with a pH of 12 using different solutions in water. (b) Line calibration of the maximum absorbance versus the agave inulin concentration (mg/mL)

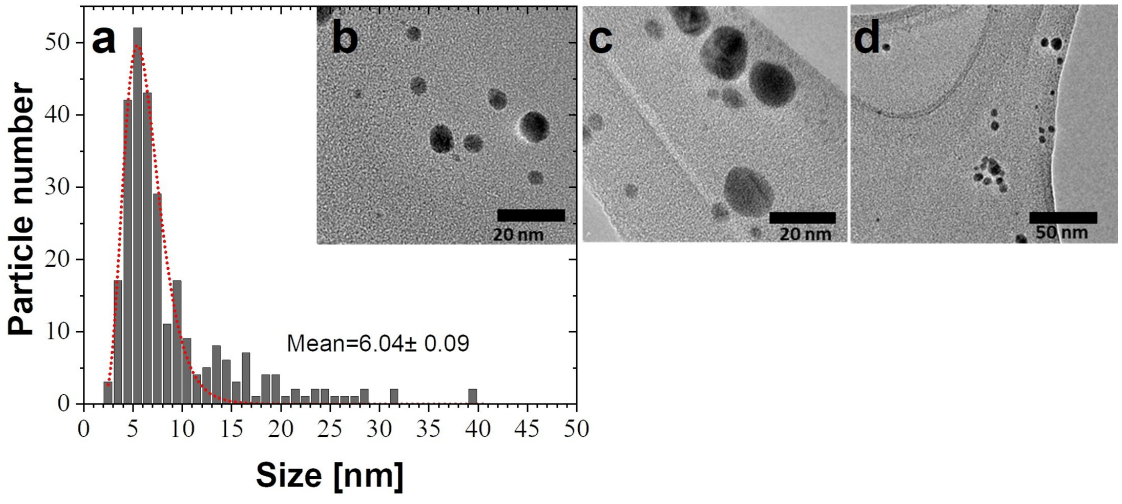

Fig. 8. (a) Size distribution, fitted with a Log-normal model (dotted line) from several micrographs (for instance b, c, and d) of AgNPs obtained using pH 11

to consider the effect of storage time, because a sample used immediately will employ a smaller concentration than expected.

3.5. Antibacterial activity

It has been reported that bactericidal properties depend on nanoparticle size; for instance, if the silver nanoparticles have a diameter of ≈1–10 nm, they present a direct interaction with the bacteria [32]. In addition, the concentration of this type of nanoparticle is another characteristic that affects bacterial growth [33, 34].

In this study, two samples, $S1_{bac}$ and $S2_{bac}$, were prepared with a molar concentration of 10 mM and 1 mM of $AgNO_3$ in dissolution with 60 mg/mL and 20 mg/mL of agave inulin, respectively. Each one was fixed to a pH of 12 and were prepared at the same temperature (see Section 2.5

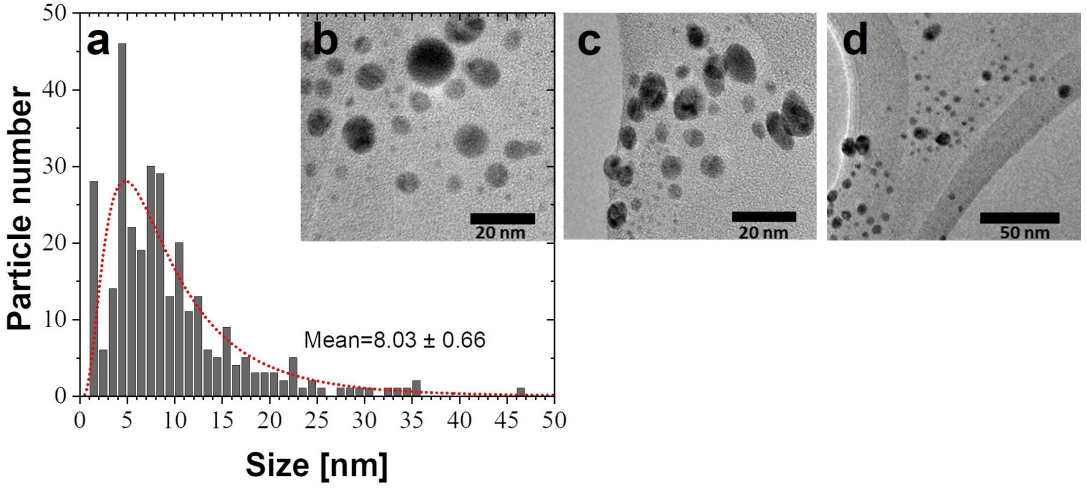

Fig. 9. (a) Size distribution, fitted with a Log-normal model (dotted line) from several micrographs (for instance b, c, and d) of AgNPs obtained using pH 10

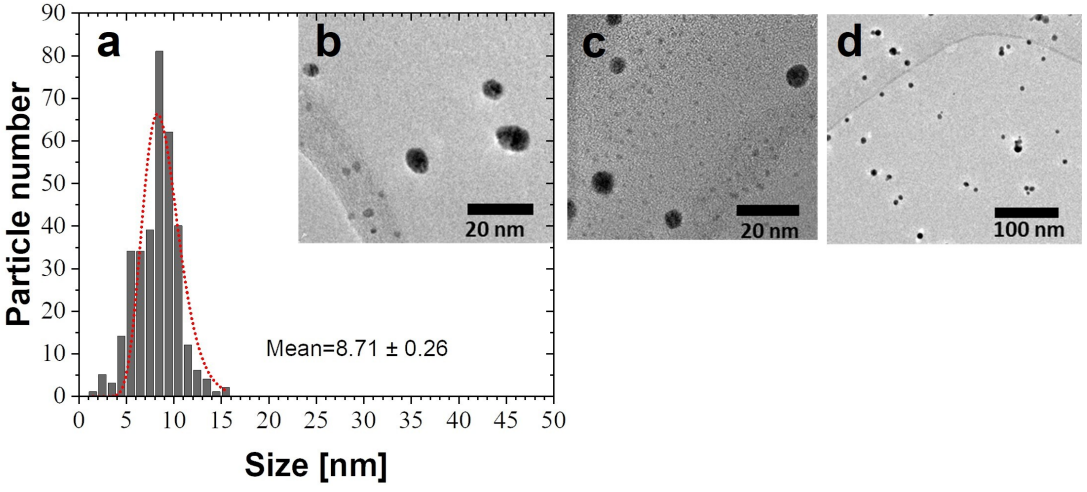

Fig. 10. (a) Size distribution, fitted with a Log-normal model (dotted line) from several micrographs (for instance b, c, and d) of AgNPs obtained using a pH of 12

for details of the preparation). Considering that the sample $S1_{bac}$ showed an antibacterial effect, consequently, the next theoretical consideration was made to determine a nanoparticle concentration (nanoparticles/mL).

For this, it is necessary to know the average size of the nanoparticle, which can be estimated from analysis of the micrographs taken by TEM. Figure 10 presents the size distribution and three micrographs of the sample $S1_{bac}$. Several nanoparticles smaller than 10 nm can be observed. If the average size of $D_p = 8.71$ nm and assuming that the nanoparticle has a spherical shape, its mass can be written as $m_p = \frac{\pi}{6} D_P^3 \ \rho_{Ag}$, where ρ_{Ag} represents the silver density (10.49 g·cm^{-3}). Substituting the density and the particle diameter, $m_p = 3.6 \times 10^{-15}$ mg is obtained.

The concentration of silver in the sample is given by $C_{Ag} = MW_{Ag} C_{AgNO_3}$, where MW_{Ag} is the atomic weight of silver (107.8682 g·mol^{-1}) and

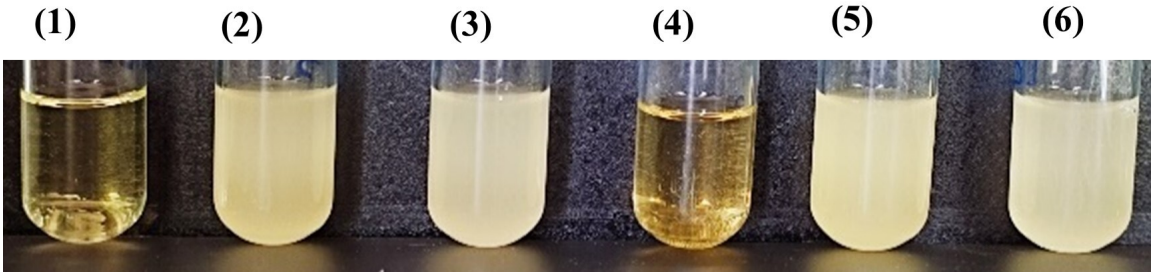

Fig. 11. Bactericidal effect. LB medium was used to determine the bactericidal effect. (1) Positive control: LB medium; (2) Negative control: LB medium and 100 μL *E. coli* strain; (3) LB medium, 100 μL *E. coli* strain, and 100 μL agave inulin; (4) LB medium, 100 μL of *E. coli* strain, and 100 μL of AgNPs ($S1_{bac}$); (5) LB medium, 100 μL of *E. coli* strain, and 100 μL of AgNPs ($S2_{bac}$); (6) LB medium, 100 μL *E. Coli* strain, and 100 μL agave inulin

C_{AgNO_3} is the concentration of $AgNO_3$ (10 mM). Substituting as seen above, $C_{Ag} = 1.07\ mg{\cdot}mL^{-1}$ is obtained. Furthermore, dividing this concentration by the average mass, the nanoparticle concentration of $\approx 2.9 \times 10^{14}$ nanoparticles/mL is obtained.

With this size distribution (Fig. 10) in comparison with the others, the procedure for obtaining the number of nanoparticles is more precise, because the nanoparticles present a narrower size distribution.

Figure 11 presents test tubes with dilutions to study the bactericidal effect according with the order shown in Table 5 (in the experimental section). Tube 1, containing only LB, represents the sterility group or the positive control, and tubes 2, 3, 5, and 6 show the bacterial growth. A solution of 100 μL of agave inulin was added to tubes 3, and 6 to verify the absence of the antibacterial effect by agave inulin. In addition, 100 μL of $S1_{bac}$ and $S2_{bac}$ were added to tubes 4 and 5, respectively. Tube 4 showed a clear bactericidal effect on the *E. coli* bacterium because there was not observed turbidity. This indicated that the sample $S1_{bac}$ caused the damage to the bacterium where this sample was prepared with the highest concentration of $AgNO_3$; hence, the concentration of silver nanoparticles had an effect against the *E. coli*. In consequence, sample $S1_{bac}$ is going to be used for further analysis against the *E. coli* bacterium.

Although the bactericidal mechanisms of silver ions are not well understood, it is inferred that they include binding and interaction mechanisms of silver nanoparticles with the cell wall and membrane [35]. It has been shown that there is electrostatic attraction between the negatively charged cell membrane of the bacteria and the positively charged silver nanoparticles, so the bactericidal activity is directly related to the positive charge of the silver ions [36, 37].

The bactericidal activity of AgNPs has been reported on Gram-negative bacteria such as *E. coli*. In this case, the concentration of silver nanoparticles is related to the formation of "holes" in the bacterial cell wall, and the accumulation of AgNPs in the cell membrane is related to the increase in the permeability of the bacterium, which triggers its death [38]. Another mechanism suggests that silver depletion could trigger the progressive release of lipopolysaccharides and cell membrane proteins, leading to the formation of "holes" [39]. It has also been proposed that silver ions released from silver nanoparticles can inactivate DNA replication and cause inhibition of enzyme functions as a result of their interaction with phosphorus moieties in DNA [40].

4. Conclusions

Silver nanoparticles were prepared in agave inulin using an eco-friendly, economical, and simple method.

According to the position and intensity of the absorption peak, high nanoparticle formation was obtained in 40 minutes using 20 mg/mL of agave

inulin, 1 mM of $AgNO_3$, at T = 23°C and pH = 12. Nevertheless, a significant bactericidal effect was obtained with the sample containing 60 mg/mL of agave inulin, 10 mM of $AgNO_3$, and the same temperature and pH.

Acknowledgements

Authors want to thank the technical assistance of Francisco Ruiz Medina and Daniel Barron Pastor with the TEM (CNYN-UNAM)). As well as financial support from Universidad de Guadalajara under programs pro-SNI and PROINPEP; María Teresa Sánchez Vieyra wants to thank National Council of Science and Technology (CONACYT-México) for its PhD scholarships.

References

[1] Mishra S, Singh HB. Biosynthesized silver nanoparticles as a nanoweapon against phytopathogens: exploring their scope and potential in agriculture. *Appl Microbiol Biotechnol.* 2015;99(3):1097–107. doi: 10.1007/s00253-014-6296-0

[2] Sánchez-Rojo SA, Martínez-Zerega BE, Velázquez-Pedroza EF, Martínez-Espinosa J. C, Torres-González L. A, Aguilar-Lemarroy A, et al. Cervical cancer detection based on serum sample surface enhanced Raman spectroscopy. *Rev Mex Fis.* 2016;62(3):213–8.

[3] Téllez GL, Luckie RAM, Mejía OFO, Mendieta VS, Reyes JT, Guerrero VV, et al. *Nanoestructuras metálicas.* 1st ed. México: Reverté; 2013.

[4] Firdhouse MJ, Lalitha P. Biosynthesis of silver nanoparticles and its applications. *J Nanotechnol.* 2015;2015: 1–18. doi: 10.1155/2015/829526

[5] Ahmed S, Ahmad M, Swami BL, Ikram S. A review on plants extract mediated synthesis of silver nanoparticles for antimicrobial applications: a green expertise. *J Adv Res.* 2016;7(1):17–28. doi: 10.1016/j.jare.2015.02.007

[6] Gardea-Torresdey JL, Gomez E, Peralta-Videa JR, Parsons JG, Troiani H, Jose-Yacaman M. Alfalfa sprouts: a natural source for the synthesis of silver nanoparticles. *Langmuir.* 2003;19(4):1357–61. doi: 10.1021/la020835i

[7] Poulose S, Panda T, Nair PP, Theodore T. Biosynthesis of silver nanoparticles. *J Nanosci Nanotechnol.* 2014;14(2):2038–49. doi: 10.1166/jnn.2014.9019

[8] Bordoloi M, Sahoo RK, Tamuli KJ, Saikia S, Dutta PP. Plant extracts promoted preparation of silver and gold nanoparticles: a systematic review. *Nano.* 2020;15(02):1–24. doi: 10.1142/S1793292020300017

[9] Oseguera-Galindo DO, Oceguera-Contreras E, Pozas-Zepeda D. Silver nanoparticles synthesis using biomolecules of habanero pepper (*Capsicum chinense* Jacq.) as a reducing agent. *J Nat Prod.* 2020;14(3): 036012–036012. doi: 10.1117/1.JNP.14.036012

[10] Justo MB, Oropeza LG, Hernández RS, Negrete LP. Azúcares en agaves (Agave tequilana Weber) cultivados en el estado de Guanajuato. *Acta Univ.* 2001;11(1):33–8. doi: http://www.redalyc.org/articulo.oa?id=41611105

[11] Handa C, Goomer S, Siddhu A. Physicochemical properties and sensory evaluation of fructoligosaccharide enriched cookies. *J Food Sci.* 2012;49(2):192–9. doi: 10.1007/s13197-011-0277-4

[12] Sánchez-Vieyra MT. Estudio de condiciones físicas y químicas en la biosíntesis de nanopartículas de plata usando infusión de chía (*Salvia hispánica*) e *inulina de agave*. Master's Degree Thesis. Guadalajara, México: University of Guadalajara; 2020.

[13] Hughes SR, Qureshi N, López-Núñez JC, Jones MA, Jarodsky JM, Galindo-Leva LA, et al. Utilization of inulin-containing waste in industrial fermentations to produce biofuels and bio-based chemicals. *World J Microbiol Biotechnol.* 2017;33(78):1–15. doi: 10.1007/s11274-017-2241-6

[14] Barclay T, Ginic-Markovic M, Cooper P, Petrovsky N. Inulin-a versatile polysaccharide: use as food chemical and pharmaceutical agent. *J Excip Food Chem.* 2010;1(3):27–50.

[15] Montañez-Soto J, Venegas-González J, Vivar-Vera M, Ramos-Ramírez E. Extracción, caracterización y cuantificación de los fructanos contenidos en la cabeza y en las hojas del Agave tequilana Weber azul. *Bioagro.* 2011;23(3):199–206.

[16] Lara-Fiallos M, Lara-Gordillo P, Julián-Ricardo MC, Pérez-Martínez A, Benítes-Cortés I. Avances en la producción de inulina. *Tecnología Química.* 2017;37(2): 352–66.

[17] Parvekar P, Palaskar J, Metgud S, Maria R, Dutta S. The minimum inhibitory concentration (MIC) and minimum bactericidal concentration (MBC) of silver nanoparticles against *Staphylococcus aureus*. *Biomater Investig Dent.* 2020;7(1):105–9. doi: 10.1080/26415275.2020.1796674

[18] Agnihotri S, Mukherji S, Mukherji S. Size-controlled silver nanoparticles synthesized over the range 5–100 nm using the same protocol and their antibacterial efficacy. *Rsc Adv.* 2014;4(8):3974–83. doi: 10.1039/c3ra44507k

[19] Oseguera-Galindo DO, Ceja-Andrade I, Martínez-Benítez A, Gómez Rosas G, Chávez-Chávez A, Pérez-Centeno A, Santa-Aranda MA. Overlapping of laser pulses and its effect on the yield of silver nanoparticles in water. *J Mater Sci Eng B.* 2014;4(10):279–83. doi: 10.17265/2161-6221/2014.10.002

[20] Haiss W, Thanh NT, Aveyard J, Fernig DG. Determination of size and concentration of gold nanoparticles from UV-Vis spectra. *Anal Chem.* 2007;79(11):4215–21. doi: 10.1021/ac0702084

[21] Krishnaraj C, Ramachandran R, Mohan K, Kalaichelvan PT. Optimization for rapid synthesis of silver nanoparticles and its effect on phytopathogenic fungi. Spectrochim. *Acta A Mol Biomol.* 2012;93:95–9. doi: 10.1016/j.saa.2012.03.002

[22] Baghizadeh A, Ranjbar S, Gupta VK, Asif M, Pourseyedi S, et al. Green synthesis of silver

nanoparticles using seed extract of *Calendula officinalis* in liquid phase. *J Mol Liq.* 2015;207:159–63. doi: 10.1016/j.molliq.2015.03.029

[23] Verma A, Mehata MS. Controllable synthesis of silver nanoparticles using Neem leaves and their antimicrobial activity. *J Radiat Res Appl Sci.* 2016;9(1):109–15. doi: 10.1016/j.jrras.2015.11.001

[24] Jain S, Mehata MS. Medicinal plant leaf extract and pure flavonoid mediated green synthesis of silver nanoparticles and their enhanced antibacterial property. *Sci Rep.* 2017;7(1):1–13. doi: 10.1038/s41598-017-15724-8

[25] Findley ME. Modified one-at-a-time optimization. *AIChE J.* 1974;20(6):1154–60. doi: 10.1002/aic.690200614

[26] Bhowmik S, Das T, Ghosh S, Sharma BK, Majumdar S, De UC. Synthesis of some new chrysin derivatives and their biological assessment as antibacterial, antibiofilm and antifungal agents. *Asian J. Chem.* 2018;30(3):693–702. doi: 10.14233/ajchem.2018.21167

[27] Oseguera-Galindo DO, Martinez-Benitez A, Chavez-Chavez A, Gomez-Rosas G, Perez-Centeno A, Santana-Aranda MA. Effects of the confining solvent on the size distribution of silver NPs by laser ablation. *J Nanopart Res.* 2012;14(9):1–6. doi: 10.1007/s11051-012-1133-9

[28] Autino JC, Romanelli GP, Ruiz DM. Introducción a la química orgánica. 1st ed. La Plata: Editorial de la Universidad Nacional de La Plata (EDULP); 2013.

[29] Zhang W, Xu W, Li J, Liu H, Li Y, Lou Y, et al. Comparative catalytic and bacteriostatic properties of silver nanoparticles biosynthesized using three kinds of polysaccharide. *AIP Adv.* 2018;8(6):1–8. doi: 10.1063/1.5034479

[30] Marciniak L, Nowak M, Trojanowska A, Tylkowski B, Jastrzab R. The effect of pH on the size of silver nanoparticles obtained in the reduction reaction with citric and malic acids. *Materials.* 2020;13(23):1–12. doi: 10.3390/ma13235444

[31] Herrera E, Álvarez MDPR, Salom PR, Arribas MV. *Bioquímica básica.* 1st ed. España SL: Elsevier; 2014.

[32] Morones JR, Elechiguerra JL, Camacho A, Holt K, Kouri JB, et al. The bactericidal effect of silver nanoparticles. *Nanotechnology.* 2005;16(10):2346–53. doi: 10.1088/0957-4484/16/10/059

[33] Ma L, Su W, Liu J-X, Zeng X-X, Huang Z, Li W, et al. Optimization for extracellular biosynthesis of silver nanoparticles by *Penicillium aculeatum* Su1 and their antimicrobial activity and cytotoxic effect compared with silver ions. *Mater Sci Eng.* 2017;77:963–71. doi: 10.1016/j.msec.2017.03.294

[34] Maldonado-Vega M, Guzmán D, Camarena-Pozos DA, Castellanos-Arévalo AP, Salinas Ramírez A, Garibo D, Bogdanchikova N. Application of silver nanoparticles to reduce bacterial growth on leather for footwear manufacturing. *J Appl Res. Technol.* 2021;19(1):41–8.

[35] Kim JS, Kuk E, Yu KN, Kim JH, Park SJ, Lee HJ, et al. Antimicrobial effects of silver nanoparticles. *Nanomed Nanotechnol Biol Med.* 2007;3(1):95–101. doi: 10.1016/j.nano.2006.12.001

[36] Dibrov P, Dzioba J, Gosink KK, Häse CC. Chemiosmotic mechanism of antimicrobial activity of Ag^{+} in *Vibrio cholerae*. Antimicro. *Agents Chemother.* 2002;46(8):2668–70. doi: 10.1128/AAC.46.8.2668-2670.2002

[37] Hamouda T, Myc A, Donovan B, Shih AY, Reuter JD, Baker JR. A novel surfactant nanoemulsion with a unique non-irritant topical antimicrobial activity against bacteria, enveloped viruses and fungi. *Microbiol Res.* 2001;156(1):1–7. doi: 10.1078/0944-5013-00069

[38] Sondi I, Salopek-Sondi B. Silver nanoparticles as antimicrobial agent: a case study on *E. Coli* as a model for Gram-negative bacteria. *J Colloid Interface Sci.* 2004;275(1):177–82. doi: 10.1016/j.jcis.2004.02.012

[39] Amro NA, Kotra LP, Wadu-Mesthrige K, Bulychev A, Mobashery S, Liu GY. High-resolution atomic force microscopy studies of the *Escherichia coli* outer membrane: structural basis for permeability. *Langmuir.* 2000;16(6):2789–96. doi: 10.1021/la991013x

[40] Gupta P, Bajpai M, Bajpai SK. Investigation of antibacterial properties of silver nanoparticle-loaded poly (acrylamide-co-itaconic acid)-grafted cotton fabric. *J Cotton Sci.* 2008;12(3):280–6.

Received 2023-07-03
Accepted 2023-11-25